

# VAE-QWGAN: Improving Quantum GANs for High Resolution Image Generation

Aaron Mark Thomas , Sharu Theresa Jose

School of Computer Science, University of Birmingham, Birmingham B15 2TT, UK  
amt326@student.bham.ac.uk, s.t.jose@bham.ac.uk

**Abstract**—This paper presents a novel hybrid quantum generative model, the VAE-QWGAN, which combines the strengths of a classical Variational AutoEncoder (VAE) with a hybrid Quantum Wasserstein Generative Adversarial Network (QWGAN). The VAE-QWGAN integrates the VAE decoder and QGAN generator into a single quantum model with shared parameters, utilizing the VAE’s encoder for latent vector sampling during training. To generate new data from the trained model at inference, input latent vectors are sampled from a Gaussian Mixture Model (GMM), learnt on the training latent vectors. This, in turn, enhances the diversity and quality of generated images. We evaluate the model’s performance on MNIST/Fashion-MNIST datasets, and demonstrate improved quality and diversity of generated images compared to existing approaches.

**Index Terms**—Quantum Machine Learning, Generative Modelling, Variational Inference

## I. INTRODUCTION

Recent advancements in quantum technology, marking the onset of the Noisy Intermediate Scale Quantum (NISQ) era of quantum devices [1], have catalyzed the field of quantum machine learning (QML) [2]. QML seeks to harness the power of quantum computing to enhance learning from classical (e.g. images) and quantum (e.g., arising from quantum sensing) data with the hope of achieving practical advantages over classical machine learning. Within this domain, quantum generative modelling has emerged as a promising sub-field, employing quantum models to learn the underlying distribution of unlabelled classical/quantum data to generate high-quality synthetic samples [3].

This paper focuses on Quantum Generative Adversarial Networks (QGANs), a class of quantum generative models that can learn both discrete [4] and continuous data distributions [5], [6]. Similar to classical GANs [7], QGANs consist of a generator network that maps latent random vectors to the data space, and a discriminator network that distinguishes between real and generated samples. These models can be fully quantum [8], [9], with both the generator and discriminator being quantum models, or hybrid, combining a quantum generator with a classical discriminator [10]. While QGANs have been effectively applied to quantum tasks such as quantum state generation [11] and quantum state loading [4], a key challenge remains: generative learning of high-dimensional classical datasets within NISQ device constraints.

In this context, hybrid QGANs, which combine quantum and classical computational paradigms, show particular promise. Notably, Huang et. al [12] introduced a hybrid *patch-QGAN*, that uses a generator consisting of multiple, quantum sub-generators each producing a patch of the output image,

and experimentally demonstrated its performance on superconducting quantum processors for generating hand-written digits. This approach was extended to develop the *patch-quantum Wasserstein GAN* (PQWGAN) [10] to generate high-dimension samples from the MNIST/Fashion-MNIST, with its performance comparable to classical models while using fewer trainable parameters. However, PQWGAN suffer from two key issues: low-quality samples and mode collapse, where the model fails to generate diverse images within the same class. Subsequent works [13] and [14] have attempted to address these drawbacks. While [13] proposes to learn on a lower-dimensional feature space, derived through principal component analysis of input pixel space, reference [14] implements generative learning in the latent space defined via the encoder of a classical AutoEncoder(AE), with the generated latent space vector remapped to the data space via the decoder.

Different from previous approaches and inspired by the classical literature [15], we introduce a novel *VAE-QWGAN* model, which combines the strengths of classical Variational AutoEncoder (VAE) with a hybrid Wasserstein QGAN. Unlike [13] and [14], our model does not require downscaling/pre-processing of input images. Specifically, VAE-QWGAN integrates the VAE decoder and QGAN generator into a single quantum model with shared parameters and use the VAE’s encoder to sample latent random vectors for the QGAN generator during training. This approach extends QGANs with a variational prior defined by the VAE, ensuring that the latent manifold is closely aligned to that of the true data. Moreover, differently from [15], we use a Gaussian mixture model (GMM) based inference to generate data from the trained model: Latent vectors are sampled from a GMM learnt on the latent vectors used during training. This, in turn, enhances the diversity and quality of the generated images. We empirically evaluate the performance of our hybrid VAE-QWGAN on MNIST/Fashion-MNIST datasets.

## II. HYBRID VAE-QWGAN MODEL

In this section, we start by providing a brief overview of the conventional classical VAE and the hybrid QGAN generative models. We then introduce our proposed VAE-QWGAN model for generating high-diversity images.

### A. Variational AutoEncoder Model

VAE [16] is a latent variable model aimed at maximising the likelihood of a parameterized distribution  $p_\theta(\mathbf{x})$  that approximates the unknown distribution  $p_r(\mathbf{x})$  underlying the observed data samples  $\mathcal{D} = \{\mathbf{x}_i\}_{i=1}^N$ . A typical (classical) VAE consists

of two networks: (a) an *encoder* network, parameterized by  $\omega$ , that defines the conditional distribution  $q_\omega(\mathbf{z}|\mathbf{x})$  of encoding the input data  $\mathbf{x}$  into a lower-dimensional latent representation  $\mathbf{z}$ , and (b) a *decoder* network, parameterized by  $\theta$ , that defines the conditional distribution  $p_\theta(\mathbf{x}|\mathbf{z})$  of decoding the latent vector  $\mathbf{z}$  to the data space. Furthermore, VAE regularizes the encoder by imposing a prior distribution  $p(\mathbf{z})$  over the latent space. Typical implementations of VAE use a Gaussian prior  $\mathcal{N}(0, \mathbb{I})$  and encoder  $q_\omega(\mathbf{z}|\mathbf{x}) = \mathcal{N}(\mu_\omega, \sigma_\omega^2 \mathbb{I})$  with  $(\mu_\omega, \log \sigma_\omega^2)$  determined by neural networks with parameters  $\omega$ .

VAE aims to minimize the negative evidence lower bound,

$$\begin{aligned} \mathcal{L}_{\text{VAE}}(\omega, \theta) &= -\mathbb{E}_{\mathbf{x} \sim p_r(\mathbf{x})} \mathbb{E}_{\mathbf{z} \sim q_\omega(\mathbf{z}|\mathbf{x})} \left[ \log \frac{p_\theta(\mathbf{x}|\mathbf{z})p(\mathbf{z})}{q_\omega(\mathbf{z}|\mathbf{x})} \right] \\ &= \mathcal{L}_{\text{recon}}(\omega, \theta) + \mathcal{L}_{\text{prior}}(\omega), \end{aligned} \quad (1)$$

where the reconstruction loss  $\mathcal{L}_{\text{recon}}(\omega, \theta)$  and the prior regularisation term  $\mathcal{L}_{\text{prior}}(\omega)$  are defined as

$$\mathcal{L}_{\text{recon}}(\omega, \theta) = -\mathbb{E}_{\mathbf{x} \sim p_r(\mathbf{x})} \mathbb{E}_{\mathbf{z} \sim q_\omega(\mathbf{z}|\mathbf{x})} [\log p_\theta(\mathbf{x}|\mathbf{z})] \quad (2)$$

$$\mathcal{L}_{\text{prior}}(\omega) = \mathbb{E}_{\mathbf{x} \sim p_r(\mathbf{x})} [D_{\text{KL}}(q_\omega(\mathbf{z}|\mathbf{x}) \| p(\mathbf{z}))], \quad (3)$$

with  $D_{\text{KL}}(p \| q)$  denoting the Kullback-Leibler divergence between two distributions  $p$  and  $q$ .

### B. Hybrid Quantum-Classical Wasserstein GAN (WQGAN)

A hybrid quantum-classical Wasserstein GAN consists of two networks: (a) a *quantum generator*  $G_\theta(\mathbf{z})$ , implemented via a variational quantum circuit (see Section III-A), that maps the latent representation  $\mathbf{z}$  to the data space, and (b) a classical neural-network based *discriminator* or *critic* network  $D_\phi(\cdot)$  that assigns a critic score to its input – either true or generated data – based on its quality. Together the generator and the critic play a min-max game, with the generator aiming to generate data that can fool the critic, and the critic aiming to efficiently separate the critic scores of the real and generated data.

Under the assumption that the family of parameterised critic functions  $\{D_\phi\}_\phi$  are 1-Lipschitz continuous, the min-max optimisation problem for the Wasserstein QGAN is defined as [17]

$$\min_{\theta} \max_{\phi} \mathcal{L}_{\text{QGAN}}(\theta, \phi) \quad \text{where,}$$

$$\mathcal{L}_{\text{QGAN}}(\theta, \phi) = \mathbb{E}_{\mathbf{x} \sim p_r(\mathbf{x})} [D_\phi(\mathbf{x})] - \mathbb{E}_{\mathbf{z} \sim p(\mathbf{z})} [D_\phi(G_\theta(\mathbf{z}))], \quad (4)$$

where  $p(\mathbf{z})$  denotes a prior distribution on the latent space. In practice, the 1-Lipschitz assumption is enforced by regularizing  $\mathcal{L}_{\text{QGAN}}(\theta, \phi)$  with a gradient penalty term as [18]

$$\begin{aligned} \mathcal{L}_{\text{QGAN-GP}}(\theta, \phi) &= \mathcal{L}_{\text{QGAN}}(\theta, \phi) \\ &+ \lambda \mathbb{E}_{\hat{\mathbf{x}} \sim \hat{p}(\mathbf{x})} \left[ (\|\nabla_{\hat{\mathbf{x}}} D_\phi(\hat{\mathbf{x}})\|_2 - 1)^2 \right]. \end{aligned} \quad (5)$$

In (5),  $\lambda$  is the penalty coefficient and  $\hat{p}(\mathbf{x}) = \epsilon p_r(\mathbf{x}) + (1 - \epsilon) p_g(\mathbf{x})$  corresponds to the distribution of points interpolated between the true distribution  $p_r(\mathbf{x})$  and generated distribution  $p_g(\mathbf{x})$ , where  $p_g(\mathbf{x})$  is defined by  $\mathbf{x} = G_\theta(\mathbf{z})$  with  $\mathbf{z} \sim p(\mathbf{z})$ , and  $\epsilon$  is sampled from uniform distribution.

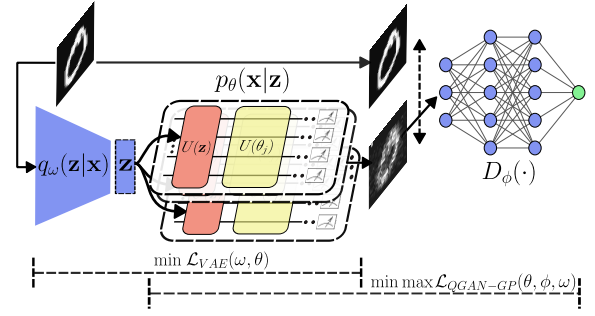


**Fig. 1:** VAE-QWGAN Schematic: The encoder  $q_\omega(\mathbf{z}|\mathbf{x})$  maps input samples  $\mathbf{x}$  to a latent variable  $\mathbf{z}$ . The decoder/generator  $p_\theta(\mathbf{x}|\mathbf{z})$  reconstructs the input image by passing through a *patch*-QGAN.

### C. Hybrid VAE-QWGAN Generative Model

Our proposed hybrid, classical-quantum VAE-QWGAN aims to improve the fidelity and diversity of the QGAN-generated data by leveraging the latent space distribution defined by a classical VAE encoder. Essentially, the hybrid VAE-QWGAN model aims to extend QGAN with a variational prior described via a VAE.

As shown in Fig. 1, the VAE-QWGAN combines the QGAN with VAE by collapsing the VAE decoder and QGAN generator, each of which maps a latent vector to the data space, into one quantum model with shared parameters  $\theta$ . Specifically, we use a Gaussian decoder  $p_\theta(\mathbf{x}|\mathbf{z}) = \mathcal{N}(G_\theta(\mathbf{z}), \mathbb{I})$  whose mean is determined by the quantum generator  $G_\theta(\mathbf{z})$ . The resulting hybrid model consists of a VAE encoder, a shared quantum decoder-generator and a classical critic. We provide details of these individual components in Section III.

1) *Training:* We train VAE-QWGAN via the combined loss,

$$\mathcal{L}(\omega, \theta, \phi) = \mathcal{L}_{\text{VAE}}(\omega, \theta) + \mathcal{L}_{\text{QGAN-GP}}(\theta, \phi, \omega), \quad (6)$$

$$\begin{aligned} \text{where } \mathcal{L}_{\text{QGAN-GP}}(\theta, \phi, \omega) &= \lambda \mathbb{E}_{\hat{\mathbf{x}} \sim \hat{p}(\mathbf{x})} \left[ (\|\nabla_{\hat{\mathbf{x}}} D_\phi(\hat{\mathbf{x}})\|_2 - 1)^2 \right] \\ &+ \mathbb{E}_{\mathbf{x} \sim p_r(\mathbf{x})} [D_\phi(\mathbf{x})] - \mathbb{E}_{\mathbf{z} \sim q_\omega(\mathbf{z}|\mathbf{x})} [D_\phi(G_\theta(\mathbf{z}))]. \end{aligned} \quad (7)$$

Importantly, distinct from the conventional QGAN training in (4) that uses latent vectors sampled from prior  $p(\mathbf{z})$ , our hybrid VAE-QWGAN uses latent vectors sampled from the VAE encoder distribution  $q_\omega(\mathbf{z}|\mathbf{x})$  (see (7)). The resulting training loss for QGAN  $\mathcal{L}_{\text{QGAN-GP}}(\theta, \phi, \omega)$  thus depends on encoder, generator and critic parameters. The training criteria in (6) can also be interpreted as an optimization of the VAE with respect to *content loss*, resulting due to the reconstruction error  $\mathcal{L}_{\text{recon}}(\omega, \theta)$ , and an additional *style loss*, resulting from the QGAN loss signal  $\mathcal{L}_{\text{QGAN-GP}}(\theta, \phi, \omega)$ .

Although the training criteria in (6) seems like a straightforward combination of the VAE and QGAN criteria, ensuring stable training requires several practical considerations:

- According to (6), the encoder training depends on the VAE loss as well as the QGAN loss, where the latter dependence is due to using the encoder distribution  $q_\omega(\mathbf{z}|\mathbf{x})$  as the prior. In practice, to ensure stable training, we dissociate signals from the QGAN and update the encoder parameters as

$$\omega \stackrel{\pm}{\leftarrow} -\nabla_{\omega} \mathcal{L}_{\text{VAE}}(\omega, \theta). \quad (8)$$

- Balancing style vs content loss: From (6), the generator is trained based on content loss-based signal from the VAE and style loss-based signals from the QGAN. To effectively balance the two losses, following [15], we use a weighing parameter  $\gamma > 0$  to balance the contribution of the respective losses to the generator parameter update:

$$\theta \stackrel{\pm}{\leftarrow} -\nabla_{\theta}(\gamma \mathcal{L}_{\text{recon}}(\omega, \theta) - \mathcal{L}_{\text{QGAN-GP}}(\theta, \phi, \omega)). \quad (9)$$

2) *Data Generation During Inference*: The training process outlined above used latent vectors sampled from the encoder distribution  $q_{\omega}(\mathbf{z}|\mathbf{x})$  to feed the generator. To generate new data from the trained hybrid VAE-QWGAN, we cannot sample latent vectors from  $q_{\omega}(\mathbf{z}|\mathbf{x})$ , since we do not have data input at inference time. Consequently, we learn a Gaussian Mixture Model  $\text{GMM}(\mu, \Sigma)$  on the latent vectors generated corresponding to each of the input training examples  $\mathbf{x}_i$  in the final training epoch. During inference, we sample vectors  $\mathbf{z} \sim \text{GMM}(\mu, \Sigma)$  to feed the generator, which outputs new data  $G_{\theta}(\mathbf{z})$ .

### III. MODEL ARCHITECTURE

In this section, we first detail the quantum generator architecture adopted in this work, followed by the encoder and critic architectures.

#### A. Quantum Generator Architecture

Since the VAE-QWGAN is designed to learn high-dimensional classical datasets, a critical challenge is the design of quantum generator architectures that can efficiently produce high-dimensional data. To this end, we adopt the patch-based generator architecture from [10], which uses a quantum generator  $G_{\theta}(\mathbf{z}) = [G_{\theta_1}(\mathbf{z}), \dots, G_{\theta_{N_g}}(\mathbf{z})]^{\top}$  that concatenates the output of  $N_g$  sub-generators.

Each  $j$ th quantum sub-generator  $G_{\theta_j}(\mathbf{z})$  is implemented via an  $n$ -qubit parameterised quantum circuit that describes an unitary operator  $U_{\theta_j}(\mathbf{z})$  acting on an initial zero state  $|0\rangle^{\otimes n} = |\mathbf{0}\rangle$  to get the quantum state  $|\psi_j(\mathbf{z})\rangle = U_{\theta_j}(\mathbf{z})|\mathbf{0}\rangle$ . In this work, we use the unitary operator of the form  $U_{\theta_j}(\mathbf{z}) = U(\theta_j)U(\mathbf{z})$  where  $U(\mathbf{z}) = \bigotimes_{i=1}^n R_y(z_i)$  is an RY-rotation-based angle encoding. This is followed by  $L$  layers of parameterized unitary gates  $U(\theta_j) = \prod_{l=1}^L W^{(l)} \bigotimes_{i=1}^n R(a_{l,i}, b_{l,i}, c_{l,i})$  (see Fig. III-A) where  $W^{(l)}$  is the CNOT-entangling, and  $R(a, b, c)$  is the general U3 operator with  $\theta_j = \{(a_{l,i}, b_{l,i}, c_{l,i}) : i = 1, \dots, n, l = 1, \dots, L\}$ .

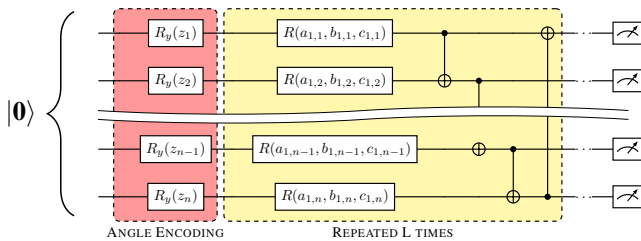


**Fig. 2:** Quantum sub-generator architecture: Hardware efficient ansatz for  $n$  qubits with RY embedding and  $L$  layers of repeated U3 rotations and strongly entangling CNOT layers.

To obtain the output  $G_{\theta_j}(\mathbf{z})$  of  $j$ th sub-generator, the quantum register is split into a set of data qubits  $n_d$  and ancillary qubits  $n_a$  such that  $n_a + n_d = n$ . We apply a non-linear projective measurement on the state  $|\psi_j(\mathbf{z})\rangle$  of the sub-generator to get the following mixed state

$$\rho_j(\mathbf{z}) = \text{Tr}_{n_a} \left( \frac{(O \otimes I) |\psi_j(\mathbf{z})\rangle \langle \psi_j(\mathbf{z})|}{\langle \psi_j(\mathbf{z}) | (O \otimes I) | \psi_j(\mathbf{z}) \rangle} \right),$$

by first applying a projective measurement of the ancillary qubit-subsystem via  $O = (|0\rangle\langle 0|)^{\otimes n_a}$ , followed by tracing it out via the partial trace operator  $\text{Tr}_{n_a}(\cdot)$ . The resulting  $\rho_j(\mathbf{z})$  is an  $n_d$ -qubit mixed state represented as a density matrix.

Computational basis measurements on the resulting mixed state  $\rho_j(\mathbf{z})$  gives an output vector

$$\tilde{\mathbf{x}}^{(j)} = [P_j(0), \dots, P_j(2^{n_d} - 1)], \quad (10)$$

where for  $k = 0, \dots, 2^{n_d} - 1$ ,  $P_j(k) = \text{Tr}(|k\rangle\langle k| \rho_j(\mathbf{z}))$  denotes the probability of measuring in the  $k$ th computational basis. Note that each component of the vector  $\tilde{\mathbf{x}}^{(j)}$  lies in the  $[0, 1]$  range since they are probabilities. We further post-process these samples to get pixel values  $G_{\theta_j}(\mathbf{z}) = \frac{\tilde{\mathbf{x}}^{(j)}}{\max_k \tilde{x}_k^{(j)}}$ . The final output vector  $G(\mathbf{z})$  is then obtained by concatenating the outputs of all  $N_g$  sub-generators.

#### B. Encoder and Critic

The encoder is a convolutional neural network with three convolutional layers that progressively reduce the spatial dimensions of the input image, extracting hierarchical features at different scales. The convolutional layer is followed by a LeakyReLU activation function [19]. The output from these convolutional layers is flattened and passed through a fully connected layer to map the high-dimensional data input into a lower-dimensional latent representation.

The critic network  $D_{\phi}(\cdot)$ , which distinguishes between real and generated images, is implemented as a dense neural network with three fully connected layers. Each layer utilises the LeakyReLU activation function to allow for better gradient flow with a 0.2 negative slope value.

### IV. EXPERIMENTAL RESULTS AND DISCUSSIONS

We now present our main findings.

*Datasets*: We use the MNIST and Fashion-MNIST datasets ( $28 \times 28 \times 1$  pixels). We randomly select 2400 training samples from two classes, specifically, the ‘0’/ ‘1’ and the ‘T-Shirt’/ ‘Trouser’ classes, from each dataset respectively.

*Network Initialization and Training*: We use a quantum generator with  $N_g = 14$  sub-generators, each consisting of  $L = 12$  layers generating patches of shape  $(2, 28)$ . Each sub-generator has  $n = 7$  qubits in total, with one ancilla qubit used for the non-linear partial measurement, yielding 3528 total parameters. The weights of each sub-generator are randomly initialized from the uniform distribution  $U_{[0, 2\pi]}$  and we evaluate (10) in the infinite shot limit. The classical encoder and critic networks use Kaiming Normal initialization for all parameters, improving stability and convergence [20]. For parameter optimisation of the VAE-QWGAN, we employ the Adam optimiser [21] with a learning rate  $lr = 0.01$  for the

decoder/generator,  $lr = 0.0003$  for the classical encoder and  $lr = 0.0005$  for the critic, with the 1st and 2nd momentum terms set as  $\beta_1 = 0$  and  $\beta_2 = 0.9$  for all optimizers. We set the style vs content loss weighing parameter to be  $\gamma = 0.0005$  following [15]. Furthermore, the gradient penalty coefficient is set as  $\lambda = 10$ . These hyperparameters are chosen empirically to assure the convergence and stability of the model. For training, we use a mini-batch size  $m = 8$  for  $n_{epochs} = 10$ , the encoder/decoder parameters are updated after every  $n_{critic} = 5$  critic parameter updates. Our code uses PyTorch [22] and PyTorch Lightning [23] packages for training algorithms implementation, and PennyLane [24] for quantum circuit construction and optimisation.

*Performance metrics:* We compare the performance of VAE-QWGAN with the state-of-the-art PQWGAN [10] that uses a Gaussian  $\mathcal{N}(0, \mathbb{I})$  and Uniform prior  $U_{[0,1]}$ . We use the sub-generator architecture shown in Fig. 2. To evaluate model performance, we track the Wasserstein distance between real and generated distributions; a lower distance indicates a better approximation of the real data sample distribution. The Jensen-Shannon Divergence (JSD) [25] and Number of Distinct Bins (NDB) score (normalised by the total number of bins, here set as 30) [26] are used to evaluate the diversity of generated images and detect mode collapse.

*Findings:* We first study the training dynamics and stability of our VAE-QWGAN compared to that of the PQWGAN that employs Gaussian and uniform priors in Fig. 3 (top row) on MNIST (left column) and Fashion-MNIST (right column) datasets. We use Wasserstein distance between the real data and the data generated during training as a performance metric and show that VAE-QWGAN achieves lower Wasserstein distance on both datasets.

In Fig. 3 (bottom row), we evaluate the reconstruction ability of our VAE-QWGAN model when fed with test images from the datasets by computing the test JSD and NDB scores. Note that reconstruction is not possible with PQWGAN as it lacks an encoder network. Consequently, we compare the test JSD/NDB with the JSD/NDB of images generated by the trained PQWGAN under both priors. The lower values of JSD and NDB scores for VAE-QWGAN is indicative of greater image diversity and less mode collapse, albeit with respect to test images. In Table 1, we evaluate these metrics on the images generated by the VAE-QWGAN with GMM-based inference. We use a GMM with 50 components.

Table 1 clearly shows that VAE-QWGAN with GMM achieves the lowest JSD and NDB scores across both datasets when compared with PQWGAN. This further indicates that the GMM approximation of the encoder latent space distribution does not in fact undermine the diversity of the images generated. We further highlight this through the images generated in Fig. 4. As can be seen from Fig. 4, the Gaussian prior produces noisy, artifact-ridden samples, with the uniform prior showing similar but less severe issues. In fact, the MNIST samples for the uniform prior highlight the generator’s difficulty in distinguishing between classes. Our VAE-QGAN model significantly improves reconstruction quality, achieving clearer class separation.

| Metric (Dataset) | Gaussian $\mathcal{N}(0, \mathbb{I})$ | Uniform $U_{[0,1]}$ | VAE-QWGAN + GMM( $\mu, \Sigma$ )   |
|------------------|---------------------------------------|---------------------|------------------------------------|
| JSD (MNIST)      | $0.28 \pm 0.036$                      | $0.19 \pm 0.033$    | <b><math>0.11 \pm 0.022</math></b> |
| JSD (F-MNIST)    | $0.38 \pm 0.014$                      | $0.33 \pm 0.038$    | <b><math>0.21 \pm 0.030</math></b> |
| NDB (MNIST)      | $0.86 \pm 0.083$                      | $0.75 \pm 0.077$    | <b><math>0.65 \pm 0.12</math></b>  |
| NDB (F-MNIST)    | $0.93 \pm 0.061$                      | $0.85 \pm 0.069$    | <b><math>0.73 \pm 0.043</math></b> |

**Table 1:** JSD and NDB scores for the images generated by the PQWGAN with uniform and Gaussian priors, and VAE-QWGAN with GMM inference after training for 10 epochs on both MNIST and Fashion-MNIST datasets. Scores are denoted as mean  $\pm$  standard deviation evaluated using 5 repeated runs of each experiment.

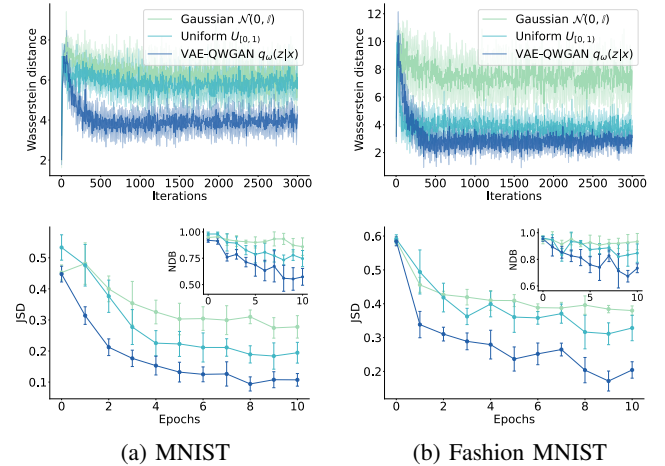


**Fig. 3:** (Top row) Evaluation of training dynamics of VAE-QWGAN and PQWGAN with uniform and Gaussian priors using Wasserstein distance on (left) MNIST and (right) Fashion-MNIST datasets. (Bottom row) Reconstruction ability of VAE-QWGAN evaluated via JSD and NDB scores computed across 2400 samples generated at the end of each training epoch. Mean and standard deviation (shaded in the top row and bars in the bottom row) evaluated on 5 experiments.

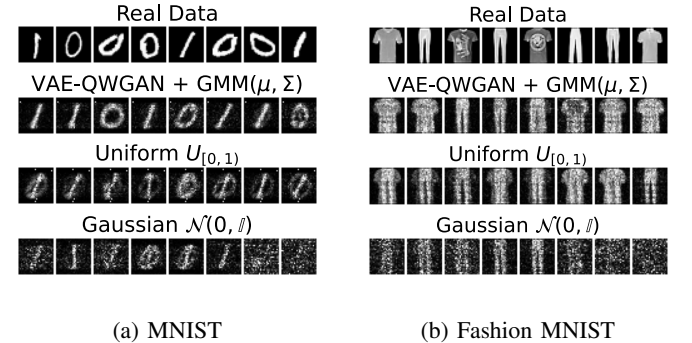


**Fig. 4:** Comparison of generated (a) MNIST samples and (b) Fashion-MNIST samples across different priors.

## V. CONCLUSION

We have demonstrated that our hybrid VAE-QWGAN outperforms the current PQWGAN approach by designing a variational prior that aligns the latent distribution with the target data, improving both the quality and diversity of generated samples. Future work will investigate how encoding methods and ansatz design affect model performance, particularly in terms of scalability and generalization to more complex datasets [27].

## REFERENCES

- [1] J. Preskill, “Quantum Computing in the NISQ era and beyond,” *Quantum*, vol. 2, p. 79, Aug. 2018.
- [2] J. Biamonte, P. Wittek, N. Pancotti, P. Rebentrost, N. Wiebe, and S. Lloyd, “Quantum machine learning,” *Nature*, vol. 549, no. 7671, pp. 195–202, 2017.
- [3] J. Tian, X. Sun, Y. Du, S. Zhao, Q. Liu, K. Zhang, W. Yi, W. Huang, C. Wang, X. Wu, M.-H. Hsieh, T. Liu, W. Yang, and D. Tao, “Recent advances for quantum neural networks in generative learning,” *IEEE Transactions on Pattern Analysis and Machine Intelligence*, vol. 45, no. 10, pp. 12321–12340, 2023.
- [4] C. Zoufal, A. Lucchi, and S. Woerner, “Quantum generative adversarial networks for learning and loading random distributions,” *npj Quantum Information*, vol. 5, no. 1, p. 103, 2019.
- [5] A. Barthe, M. Grossi, S. Vallecorsa, J. Tura, and V. Dunjko, “Expressivity of parameterized quantum circuits for generative modeling of continuous multivariate distributions,” *arXiv preprint arXiv:2402.09848*, 2024.
- [6] C. Bravo-Prieto, J. Baglio, M. Cè, A. Francis, D. M. Grabowska, and S. Carrazza, “Style-based quantum generative adversarial networks for Monte Carlo events,” *Quantum*, vol. 6, p. 777, Aug. 2022.
- [7] I. Goodfellow, J. Pouget-Abadie, M. Mirza, B. Xu, D. Warde-Farley, S. Ozair, A. Courville, and Y. Bengio, “Generative adversarial networks,” *Commun. ACM*, vol. 63, p. 139–144, oct 2020.
- [8] S. Lloyd and C. Weedbrook, “Quantum generative adversarial learning,” *Physical review letters*, vol. 121, no. 4, p. 040502, 2018.
- [9] P.-L. Dallaire-Demers and N. Killoran, “Quantum generative adversarial networks,” *Physical Review A*, vol. 98, no. 1, p. 012324, 2018.
- [10] S. L. Tsang, M. T. West, S. M. Erfani, and M. Usman, “Hybrid quantum–classical generative adversarial network for high-resolution image generation,” *IEEE Transactions on Quantum Engineering*, vol. 4, pp. 1–19, 2022.
- [11] L. Hu, S.-H. Wu, W. Cai, Y. Ma, X. Mu, Y. Xu, H. Wang, Y. Song, D.-L. Deng, C.-L. Zou, *et al.*, “Quantum generative adversarial learning in a superconducting quantum circuit,” *Science advances*, vol. 5, no. 1, p. eaav2761, 2019.
- [12] H.-L. Huang, Y. Du, M. Gong, Y. Zhao, Y. Wu, C. Wang, S. Li, F. Liang, J. Lin, Y. Xu, *et al.*, “Experimental quantum generative adversarial networks for image generation,” *Physical Review Applied*, vol. 16, no. 2, p. 024051, 2021.
- [13] D. Silver, T. Patel, W. Cutler, A. Ranjan, H. Gandhi, and D. Tiwari, “Mosaic: Quantum generative adversarial networks for image generation on nisy computers,” in *Proceedings of the IEEE/CVF International Conference on Computer Vision*, pp. 7030–7039, 2023.
- [14] S. Y. Chang, S. Thanasilp, B. Le Saux, S. Vallecorsa, and M. Grossi, “Latent Style-based Quantum GAN for high-quality Image Generation,” *arXiv e-prints*, p. arXiv:2406.02668, June 2024.
- [15] A. B. L. Larsen, S. K. Sønderby, H. Larochelle, and O. Winther, “Autoencoding beyond pixels using a learned similarity metric,” in *International conference on machine learning*, pp. 1558–1566, PMLR, 2016.
- [16] D. P. Kingma and M. Welling, “Auto-Encoding Variational Bayes,” in *2nd International Conference on Learning Representations, ICLR 2014, Banff, AB, Canada, April 14-16, 2014, Conference Track Proceedings*, 2014.
- [17] M. Arjovsky, S. Chintala, and L. Bottou, “Wasserstein generative adversarial networks,” in *Proceedings of the 34th International Conference on Machine Learning (D. Precup and Y. W. Teh, eds.)*, vol. 70 of *Proceedings of Machine Learning Research*, pp. 214–223, PMLR, 06–11 Aug 2017.
- [18] I. Gulrajani, F. Ahmed, M. Arjovsky, V. Dumoulin, and A. Courville, “Improved training of wasserstein gans,” in *Proceedings of the 31st International Conference on Neural Information Processing Systems, NIPS’17*, (Red Hook, NY, USA), p. 5769–5779, Curran Associates Inc., 2017.
- [19] B. “Xu, N. ”Wang, T. ”Chen, and M. ”Li, “Empirical evaluation of rectified activations in convolutional network,” 2015.
- [20] K. He, X. Zhang, S. Ren, and J. Sun, “Delving deep into rectifiers: Surpassing human-level performance on imagenet classification,” in *2015 IEEE International Conference on Computer Vision (ICCV)*, pp. 1026–1034, 2015.
- [21] D. Kingma and J. Ba, “Adam: A method for stochastic optimization,” in *International Conference on Learning Representations (ICLR)*, (San Diego, CA, USA), 2015.
- [22] A. Paszke, S. Gross, F. Massa, A. Lerer, J. Bradbury, G. Chanan, T. Killeen, Z. Lin, N. Gimelshein, L. Antiga, *et al.*, “Pytorch: An imperative style, high-performance deep learning library,” *Advances in neural information processing systems*, vol. 32, 2019.
- [23] W. Falcon and The PyTorch Lightning team, “PyTorch Lightning,” Mar. 2019.
- [24] V. Bergholm, J. Izaac, M. Schuld, C. Gogolin, S. Ahmed, V. Ajith, M. Sohaib Alam, G. Alonso-Linaje, B. AkashNarayanan, A. Asadi, J. M. Arrazola, U. Azad, S. Banning, C. Blank, T. R. Bromley, B. A. Cordier, J. Ceroni, A. Delgado, O. Di Matteo, A. Dusko, T. Garg, D. Guala, A. Hayes, R. Hill, A. Ijaz, T. Isaacsson, D. Ittah, S. Jahangiri, P. Jain, E. Jiang, A. Khandelwal, K. Kottmann, R. A. Lang, C. Lee, T. Loke, A. Lowe, K. McKiernan, J. J. Meyer, J. A. Montañez-Barrera, R. Moyard, Z. Niu, L. J. O’Riordan, S. Oud, A. Panigrahi, C.-Y. Park, D. Polatajko, N. Quesada, C. Roberts, N. Sá, I. Schoch, B. Shi, S. Shu, S. Sim, A. Singh, I. Strandberg, J. Soni, A. Száva, S. Thabet, R. A. Vargas-Hernández, T. Vincent, N. Vitucci, M. Weber, D. Wierichs, R. Wiersema, M. Willmann, V. Wong, S. Zhang, and N. Killoran, “PennyLane: Automatic differentiation of hybrid quantum-classical computations,” *arXiv e-prints*, p. arXiv:1811.04968, Nov. 2018.
- [25] Y. Liu and Y. Li, “Metrics of gans,” <https://github.com/yhleo/GAN-Metrics>, 2021. Accessed: 2024-09-02, Online.
- [26] E. Richardson and Y. Weiss, “On gans and gmm,” *Advances in neural information processing systems*, vol. 31, 2018.
- [27] M. Weigold, J. Barzen, F. Leymann, and M. Salm, “Data encoding patterns for quantum computing,” in *Proceedings of the 27th Conference on Pattern Languages of Programs, PLoP ’20*, (USA), The Hillside Group, 2022.